

**\*\*Volume Title\*\***  
**ASP Conference Series, Vol. \*\*Volume Number\*\***  
**\*\*Author\*\***  
 © **\*\*Copyright Year\*\*** *Astronomical Society of the Pacific*

## Pulsar Wind Nebulae from X-rays to VHE $\gamma$ -rays

Oleg Kargaltsev,<sup>1</sup> George G. Pavlov,<sup>2,3</sup> and Martin Durant<sup>1</sup>

<sup>1</sup> *University of Florida, Bryant Space Center, Gainesville, FL 32611*

<sup>2</sup> *Pennsylvania State University, 525 Davey Lab., University Park, PA 16802*

<sup>3</sup> *St.-Petersburg State Polytechnic University, 195251, Russia*

**Abstract.** The number of plausible associations of extended VHE (TeV) sources with pulsars has been steadily growing, suggesting that many of these sources are pulsar wind nebulae (PWNe). Here we overview the recent progress in X-ray and TeV observations of PWNe and summarize their properties.

Along with supernovae, pulsars produce copious amounts of relativistic particles and inject them into the Galactic medium. The energies of pulsar wind electrons and positrons range from  $\sim 1$  GeV to  $\sim 1$  PeV, placing their synchrotron and inverse Compton (IC) emission into radio-X-ray and GeV-TeV bands, respectively. This multi-wavelength emission can be seen as a *pulsar-wind nebula* (PWN) (Kargaltsev & Pavlov 2008, 2010). The wind particles can be trapped in the pulsar vicinity for  $\gtrsim 10^5$  yr, forming relic TeV PWNe, which appear to dominate the population of Galactic VHE  $\gamma$ -rays sources. Here we provide an updated overview based on a compilation of observational properties of 85 PWNe or PWN candidates, 71 of which have suggested associations with pulsars. Because of limited space, we restrict ourselves by graphical presentations and short discussions of various correlations that involve PWN luminosities and spectral slopes.

In Figure 1 we show the sample of the 71 X-ray/TeV PWNe and PWN candidates, which are likely associated with detected pulsars, in the  $\tau$ - $\dot{E}$  plane, where  $\dot{E}$  and  $\tau$  are the pulsar's spin-down power and characteristic age. This figure demonstrates that the X-ray/TeV PWNe are detectable up to an age of a few times  $10^5$  yr, and at  $\dot{E}$  as low as  $\sim 10^{34}$  erg s<sup>-1</sup>. It also demonstrates that their X-ray luminosities generally decrease with increasing age (decreasing spin-down power), while the TeV luminosities do not show an obvious dependence on these parameters.

The different correlations of the PWN TeV and X-ray luminosities,  $L_\gamma$  and  $L_X$ , with  $\dot{E}$  are demonstrated in top panels of Figures 2 and 3. X-ray luminosities exhibit a large spread (up to 4 orders of magnitude) at a given  $\dot{E}$ , which apparently grows with increasing  $\dot{E}$ . This means that there is no a unique dependence of  $L_X$  on  $\dot{E}$ , but rather the  $L_X$  values lie below an upper bound,  $L_X^{\text{cr}}(\dot{E})$ . Interestingly, the bound is about the same as that found for the nonthermal *pulsar* luminosities (Kargaltsev et al. 2012). On the contrary, the TeV luminosities do not show a significant correlation with  $\dot{E}$ , and the upper bound,  $L_\gamma^{\text{cr}} \sim 10^{35}$  erg s<sup>-1</sup>, does not show a significant dependence on the pulsar's spin-down power. Such different behavior is consistent with the interpretation of majority of TeV PWNe as relic plerions, which are powered by aged leptons, injected by the pulsar long ago, when its spin-down power was much higher. On the other

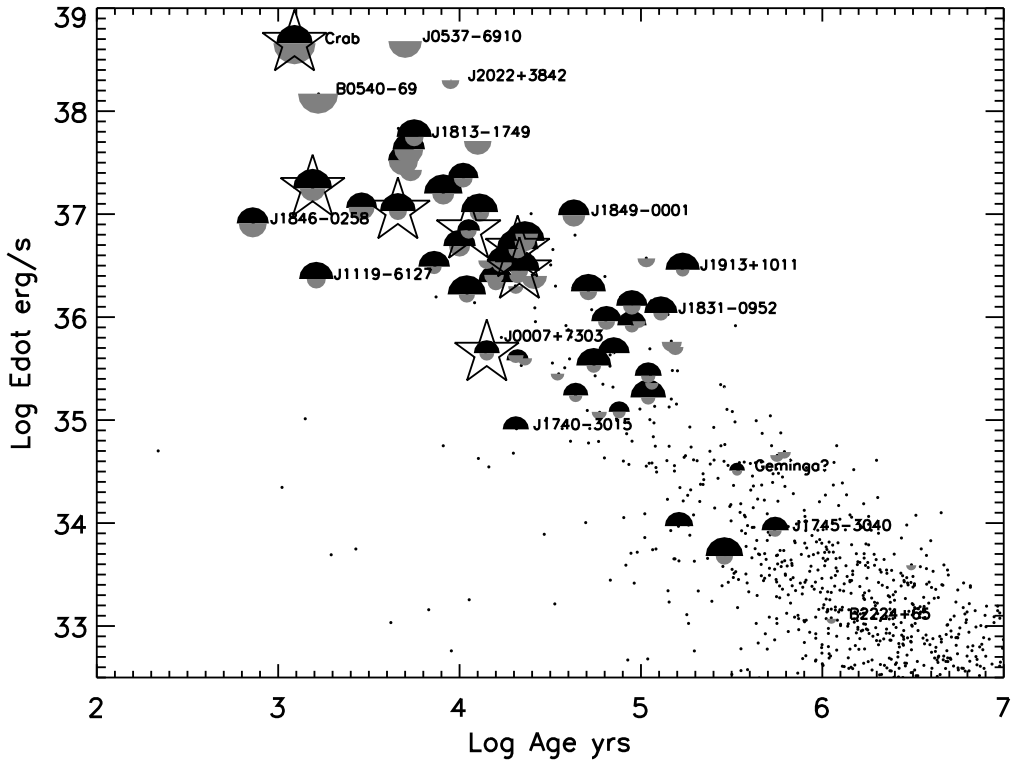


Figure 1. Pulsars with detected PWNe (or PWN candidates) in the  $\tau$ - $\dot{E}$  diagram. The semi-circles correspond to X-ray (grey) and TeV (black) PWNe, their sizes are proportional to logarithms of the PWN luminosities. The small black dots denote the pulsars from the ATNF catalog (Manchester et al. 2005). PWNe detected by *Fermi* are marked by stars.

hand,  $L_\gamma$  does not correlate significantly with the product  $\dot{E}\tau$  (Fig. 2, bottom panel), which crudely characterizes the total energy lost by the pulsar during its life time. The distance-independent ratio  $L_\gamma/L_X$  shows a hint of growth with increasing age (decreasing  $\dot{E}$ ) for young, powerful pulsars ( $\tau \lesssim 10$  kyr,  $\dot{E} \gtrsim 10^{37}$  erg s $^{-1}$  – see Fig. 4; bottom panel), which could, at least partly, be explained by the positive correlation of  $L_X$  with  $\dot{E}$ . Note that most of the detected PWNe are more luminous in TeV than in X-rays, except for 5 young objects. This trend can also be seen from the top panel of Figure 4, which includes PWN candidates yet lacking a pulsar detection.

As the spectral slopes have been measured for many PWNe in both X-ray and TeV bands, we can compare various correlations that involve the photon indices  $\Gamma_X$  and  $\Gamma_\gamma$ . First of all, the TeV spectra are generally softer than the X-ray spectra, with typical values  $\Gamma_X \approx 1.7$  and  $\Gamma_\gamma \approx 2.2$  (Fig. 5; one should remember, however, that most of the TeV PWNe are significantly larger and farther from the pulsar than their X-ray counterparts). Figure 5 (top panel) shows a lack of correlation between the spectral slopes of the X-ray and TeV PWNe. We also see no correlation between  $L_X$  and  $\Gamma_X$  (Fig. 6), while there is a hint of decreasing spread of  $\Gamma_\gamma$  with increasing  $L_\gamma$ .

The detected TeV PWNe and PWN candidates can be divided in two classes. First, relatively small, class includes very young PWNe powered by energetic pulsars (e.g.,

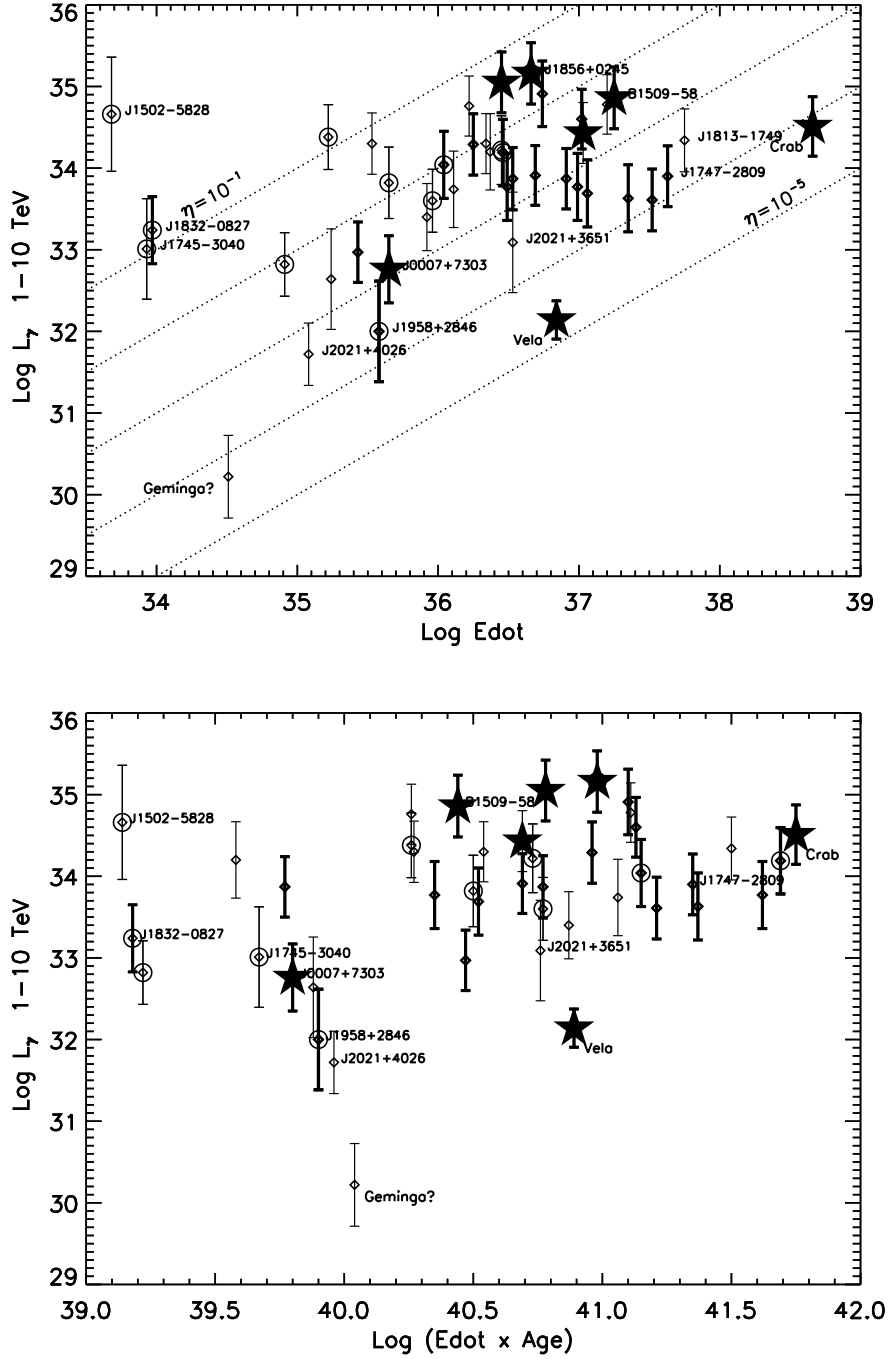


Figure 2. TeV luminosities of PWNe and PWN candidates vs. pulsar's  $\dot{E}$  (top) and  $\dot{E}\tau$  (bottom). Thin error bars mark questionable associations. PWNe undetected in X-rays are shown as circles. PWNe detected by *Fermi* are marked by stars. Dotted lines in the top panel correspond to constant values of the ratio  $\eta_\gamma = L_\gamma / \dot{E}$ .

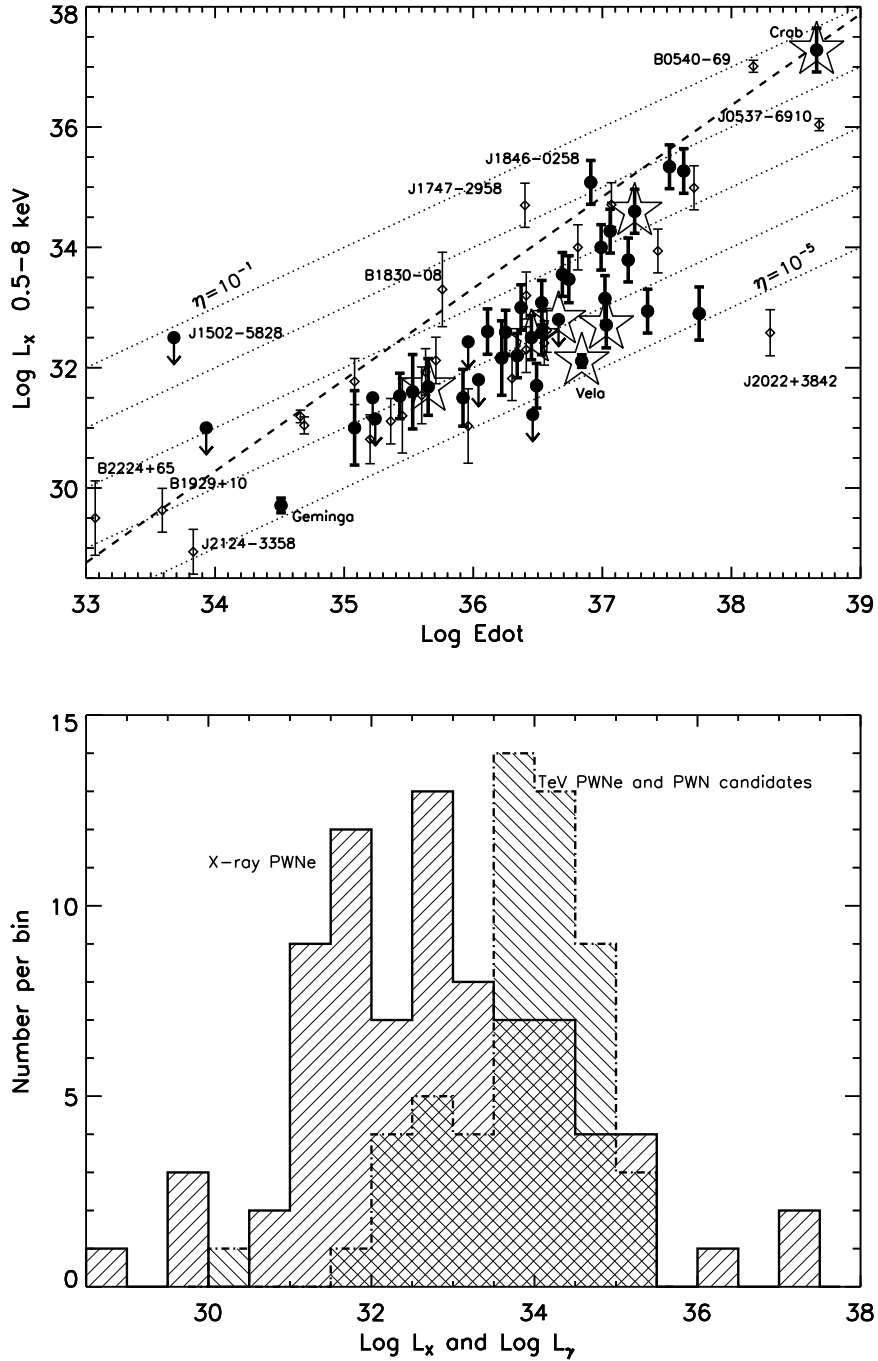


Figure 3. *Top*: X-ray luminosities of PWNe and PWN candidates vs. pulsar's  $\dot{E}$ . TeV PWNe and TeV PWN candidates are shown as filled circles. Dotted straight lines correspond to constant X-ray efficiencies; the upper bound,  $\log L_x^{\text{cr}} = 1.51 \log \dot{E} - 21.4$  (Kargaltsev et al. 2012), is shown by a dashed line. PWNe detected by *Fermi* are marked by stars. *Bottom*: Distributions of PWNe and PWN candidates over the X-ray and TeV luminosities.



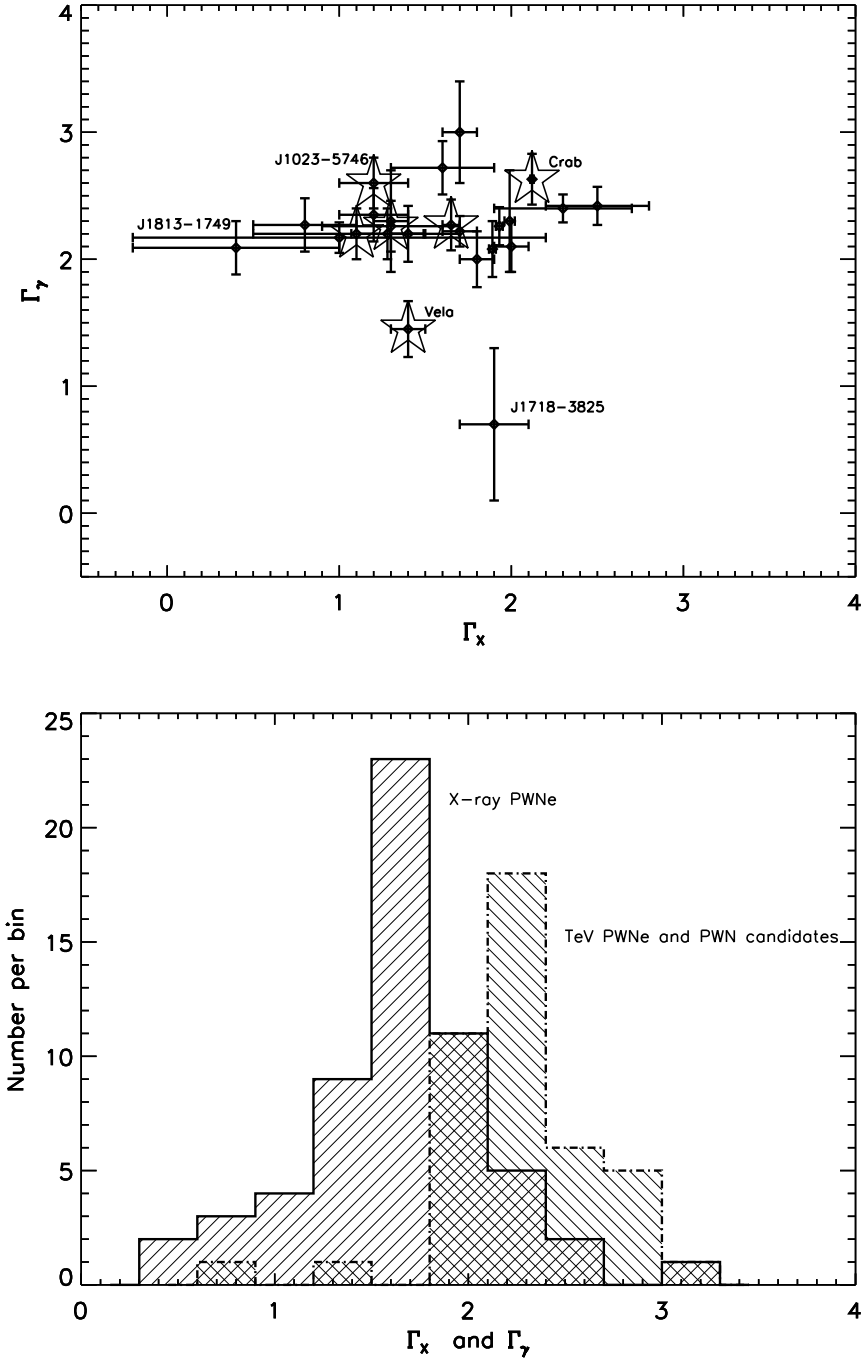


Figure 5. TeV vs. X-ray photon indices for PWNe and PWN candidates (*top*) and index distributions (*bottom*).

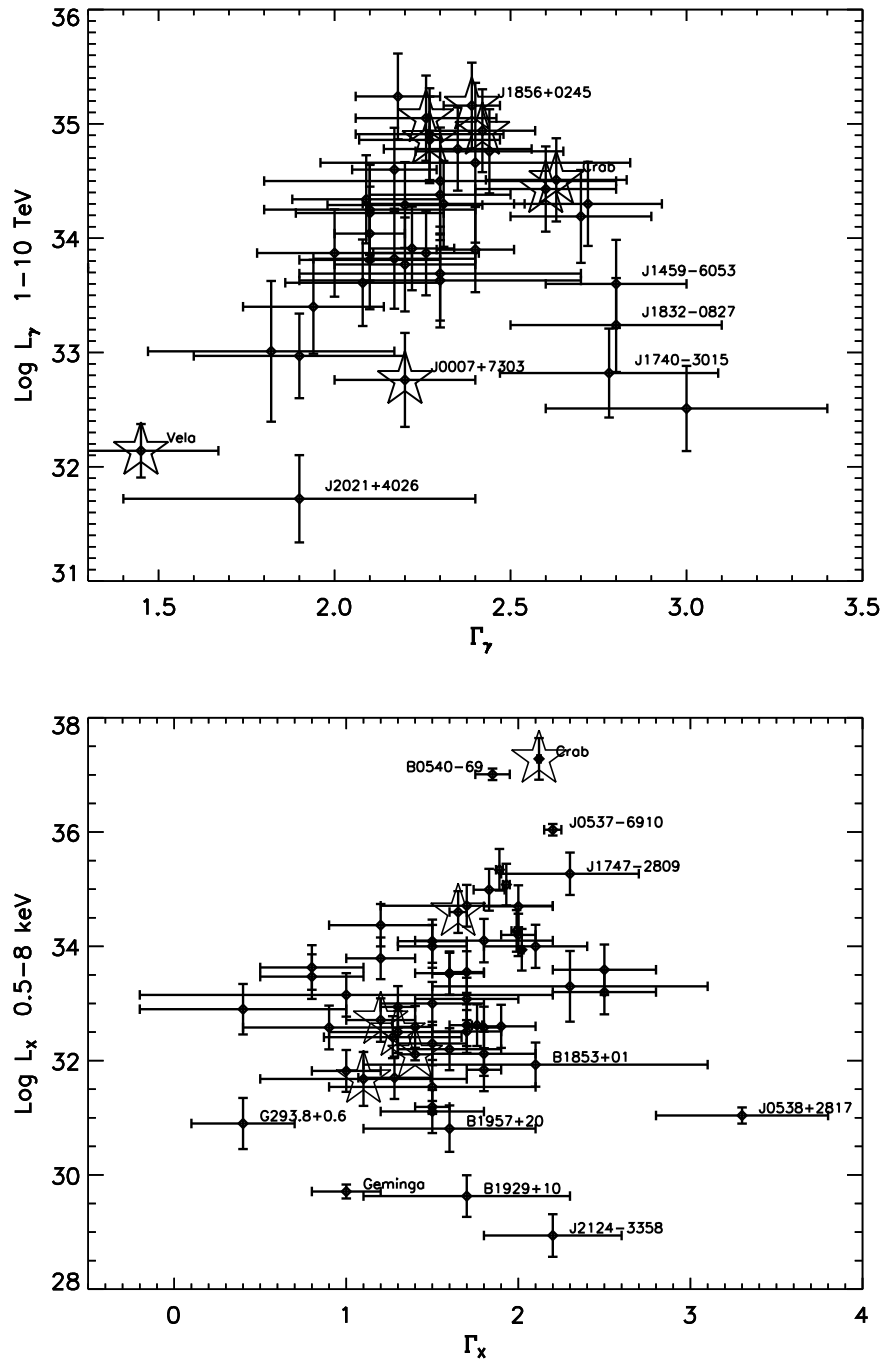


Figure 6. PWN luminosity vs. photon index in the TeV and X-ray bands. PWNe detected by *Fermi* are marked by stars.

Crab, J1833–1034, J1930+1852, J1846–0258), without significant offsets from the pulsars and X-ray PWNe, in which  $\gamma$ -rays and X-rays are likely emitted by the same population of electrons. Second class consists of older objects, in which the TeV PWNe are usually much larger than (and often strongly offset from) the X-ray PWNe (e.g., HESS J1825–137, HESS J1809–193, Vela-X). These relic TeV plerions, offset and compressed by the SNR reverse shock, are filled with aged electrons that have cooled due to synchrotron and IC energy losses; based on their properties, we can assume that they still reside inside their host SNRs (which, however, have not been detected for some of these objects).

TeV emission from PWNe created by pulsars that have escaped from their SNRs and move supersonically in the ISM have not been firmly detected yet. About a dozen of such pulsars are known to be accompanied by ram-pressure confined bow-shock PWNe with long tails often seen in X-rays and/or radio (e.g., J1747–2958, J1509–5850, B0355+54, J0633+1746, B1957+20). If the TeV production is due to a hadronic component of the pulsar wind, the nondetections might be explained by the lower ambient density. In case of purely leptonic pulsar wind, bow-shock TeV PWNe, which might be created by the freshly shocked electrons in the pulsar vicinity, are perhaps too faint because of lower spin-down powers of these relatively old pulsars. A possible explanation of nondetections of the long, up to 12'–15' (or up to  $\sim 20$  pc), tails filled by the older wind particles is a lower sensitivity of the existing TeV imaging techniques to extended linear structures. It is, however, possible that the wind particles channeled into the tails behind the pulsars accumulate in lobes, which are not seen in X-rays (due to the relatively short synchrotron cooling time) but could be sources of IC TeV emission, strongly offset from the pulsar. As the surface brightness of such lobes may be relatively low, deep TeV (and/or radio) observations are required for their detection.

Multiwavelength observations of PWNe are crucial because they provide identifications for VHE sources and reveal the energetics and composition of pulsar winds. In addition to X-ray and TeV observations, the IC PWN component can be detected with *Fermi* LAT in the GeV band, where even old objects should exhibit uncooled IC spectra, matching the radio synchrotron component. The data accumulation must be complemented by development of multi-zone models of PWN evolution (Tang & Chevalier 2012), to understand the nature of pulsar winds and their role in seeding the Galaxy with energetic particles and magnetic fields.

**Acknowledgments.** This material is based upon work supported by National Science Foundation under grants AST-0908733 and AST-0908611. The work of GGP was partially supported by the Ministry of Education and Science of the Russian Federation (contract 11.G34.310001).

## References

- Kargaltsev, O., Durant, M., Pavlov, G. G., & Garmire, G. 2012, ArXiv e-prints. 1202.3838  
 Kargaltsev, O., & Pavlov, G. G. 2008, in 40 Years of Pulsars: Millisecond Pulsars, Magnetars and More, edited by C. Bassa, Z. Wang, A. Cumming, & V. M. Kaspi, vol. 983 of American Institute of Physics Conference Series, 171  
 — 2010, X-ray Astronomy 2009; Present Status, Multi-Wavelength Approach and Future Perspectives, 1248, 25  
 Manchester, R. N., Hobbs, G. B., Teoh, A., & Hobbs, M. 2005, AJ, 129, 1993  
 Tang, X., & Chevalier, R. A. 2012, ApJ, 752, 83